doi:10.3788/gzxb20154404.0406002

色散平坦渐减光纤中抽运残余成分的抑制与平坦超连续谱的产生

徐永钊[1], 宋建勋[1],凌东雄[1], 叶海[1],李洪涛[1],韩涛[1,2]
(1 东莞理工学院 电子工程学院,广东 东莞 523808)
(2 东莞中山大学研究院,广东 东莞 523808)

摘 要:基于广义非线性薛定谔方程,通过数值模拟研究了色散平坦渐减光纤中抽运残余成分的抑制.研究结果表明:超连续谱的形状由输入孤子阶数 N、归一化二次色散系数 Δ_2 和归一化有效光纤长度 ξ_0 决定.对于给定 N 和给定 Δ_2 值的抽运脉冲,超连续谱的形状依赖于 ξ_0.通过合适地选取 ξ_0,抽运残余成分可以被有效地抑制并获光谱平坦度令人满意的超连续谱.为了获得参量 ξ_0 的最优值,引入了 S 因子评价超连续谱的波动.S 因子值越小,所产生的超连续谱越平坦.保持 N 和 Δ_2 不变,计算了 ξ_0 取不同值时,所产生的超连续谱的 S 因子.当 S 因子达到最小值时,抽运残余成分被抑制到最大限度,并获得最平坦的超连续谱,相应的 ξ_0 值即为归一化参量 ξ_0 的最优值.计算了 N 在 1.0~2.2 范围内,ξ_0 的最优值.结果显示当 N 降低时,ξ_0 的最优值增大.为产生具有弱残余抽运成分的超连续谱,抽运脉冲采用低阶孤子要优于高阶孤子.

关键词:非线性光学;色散平坦渐减光纤;超连续谱产生;孤子;脉冲压缩
中图分类号:TN25 **文献标识码**:A **文章编号**:1004-4213(2015)04-0406002-6

Suppression of Residual Pump Component for Flat Supercontinuum Generation in Dispersion-Flattened Dispersion-Decreasing Fibers

XU Yong-zhao[1], SONG Jian-xun[1], LING Dong-xiong[1], YE Hai[1], LI Hong-tao[1], HAN Tao[1,2]
(1 *School of Electronic Engineering, Dongguan University of Technology, Dongguan, Guangdong* 523808, *China*)
(2 *Dongguan Institute, Sun Yat-sen University, Dongguan, Guangdong* 523808, *China*)

Abstract: Numerical simulations based on generalized nonlinear Schrödinger equation were used to study the suppression of residual pump component of supercontinuum generated in dispersion-flattened dispersion-decreasing fibers. The results show that the shape of a supercontinuum spectrum is uniquely specified by the input soliton order N, the normalized quadratic dispersion coefficient Δ_2 and the normalized effective fiber length ξ_0. For a pump pulse with a given N and a given value of Δ_2, the shape of a supercontinuum spectrum depends on ξ_0. By appropriately choosing ξ_0, the residual pump component can be suppressed effectively and a supercontinuum with desirable spectral flatness can be obtained. In order to obtain the optimal value of ξ_0, S-factor is introduced to estimate the fluctuation of supercontinuum spectrum. The smaller the value of S-factor, the flatter the generated spectrum. Keeping N and Δ_2 constant, S-factor of the generated supercontinuum spectrum for different value of ξ_0 was calculated. When S-factor reaches a minimum value, the residual pump component is suppressed to the utmost extent and a flattest supercontinuum spectrum is obtained. The corresponding ξ_0 is the optimal value of ξ_0. The optimal value of ξ_0 for the pump pulses with soliton order N in the range $1.0 \leqslant N \leqslant 2.2$ was calculated. It is

Foundation item: The Guangdong Science and Technology Program (No. 2012B090600009), the Guangdong Natural Science Fund (No. 10451170003004948)
First author: XU Yong-zhao (1972—), male, associate professor, Ph. D. degree, mainly focuses on nonlinear fiber optics and optical communication techniques. Email: yongzhaoxu@126.com
Received: Aug. 26, 2014; **Accepted**: Dec. 4, 2014

found that when N decreases, the optimal value of ξ_0 increases. To generate a supercontinuum spectrum with weak residual pump component, lower-order soliton pulses are preferable to higher-order soliton pulses.

Key words: Nonlinear optics; Dispersion-flattened dispersion-decreasing fiber; Supercontinuum generation; Solitons; Pulse compression

OCIS Codes: 320.6629, 060.2310, 060.4370

0 Introduction

Supercontinuum (SC) generation in nonlinear fibers has attracted continuous research interest due to its revolutionary applications in numerous areas, such as telecommunication, spectroscopy, microscopy, and optical coherence tomography [1-4]. As a broadband light source of SC, practical applications usually favor a flatter SC spectrum. Thus far, efforts have been devoted to generating wider and flatter SC spectra. Dispersion-Flattened Dispersion-decreasing Fibers (DFDFs) [5-10], Dispersion Decreasing Fibers (DDFs)[11], conventional Dispersion Flattened Fiber (DFF) [12], Photonic Crystal Fibers (PCFs) [13-15] were proven to be successful candidates for flat wideband SC generation. Among those fibers, DFDFs have shown to be appropriate for generating flatly broadened SC spectra by using picosecond pump pulse with relatively low peak power. SC spectrum with typical bandwidths in excess of several hundreds of nanometers can be easily generated even if the peak power of the pump pulse is as low as a few-Watt. However, the problem with SC spectra generated from DFDFs is that there is a sharp peak at the pump wavelength, and much of the pump pulse energy is stored in this sharp peak[5-10]. As a result, the spectrally flat region is quite low in power. This sharp peak is typical of most of the SC spectra, and it is a manifestation of Self-Phase Modulation (SPM) effect during higher-order soliton compression in DFDF.

Many numerical studies have been carried out with the aim of better understanding the mechanisms in the SC process in DFDFs. The effects on the SC generation of input pulse properties and fiber properties have been investigated thoroughly [5-10]. However, to the best of our knowledge, how to suppress the residual pump component and improve the distribution of pump power in DFDFs has not been studied in detail. In this paper, we are presenting a numerically study of SC generation in DFDFs with the purpose of suppressing the residual pump component and improving distribution of pump power among the SC spectrum. Numerical simulations show that by appropriately choosing the fiber parameters and the pumping conditions, the strong residual pump component can be suppressed greatly and a high quality SC spectrum can be obtained.

1 Theoretical model

Here we introduce an idealized dispersion characteristic in a DFDF, $D(\lambda, z)$, expressed as

$$D(\lambda, z) = D_0\left(1-\frac{z}{L_0}\right)+\frac{D_2}{2}(\lambda-\lambda_0)^2 \tag{1}$$

where D_0 is chromatic dispersion $D(\lambda_0, 0)$ at the input. In this idealized SC fiber, chromatic dispersion $D(\lambda_0, z)$ decreases linearly with propagation distance z from positive D_0 to a negative value while maintaining a constant peak wavelength λ_0. $D_2 = (\partial^2/\partial\lambda^2)D(\lambda_0, L_0)$ has a negative value in the case of a convex dispersion profile. Effective fiber length L_0 is defined as the propagation distance after which the dispersion $D(\lambda_0, z)$ becomes negative (normal dispersion). In this paper, we assume the pump wavelength $\lambda_p = \lambda_0 = 1\,550$ nm.

We use a Generalized Nonlinear Schrödinger Equation (GNLSE) to model the pulse propagation inside the fiber. In a frame of reference moving at the group velocity of the pulse, the GNLSE can be written in its normalized form as[16]

$$\frac{\partial U}{\partial \xi} = \sum_{m=2}^{\infty} i^{m+1}\delta_m \frac{\partial^m U}{\partial \tau^m} + i\left(|U|^2 U + is\frac{\partial}{\partial \tau}|U|^2 U - \tau_R U\frac{\partial |U|^2}{\partial \tau}\right) \tag{2}$$

Here, the field amplitude $U(\xi, \tau)$ is normalized such that $U(0, 0) = 1$. The other variables are defined as

$$\begin{cases}\xi = z/L_{NL}\\ \tau = (t - z/v_g)/T_0\\ \beta_m = \left(\dfrac{d^m\beta}{d\omega^m}\right)_{\omega=\omega_0}\end{cases} \tag{3}$$

$$\delta_m = \frac{\beta_m}{m!\ \gamma P_0 T_0^m} \tag{4}$$

where T_0 is the half-width (at 1/e-intensity point), for a hyperbolic secant pulse, it related to the full width at half maximum (T_{FWHM}) by $T_{FWHM}(1.763T_0$. P_0 is the peak power of the pulse launched into the fiber, $L_{NL} = 1/(\gamma P_0)$ is the nonlinear length, v_g is the group velocity, γ is the nonlinear parameter, δ_m is the m-th order dispersion coefficient in normalized form, $s = (\omega_0 T_0)^{-1}$ is the self-steepening parameter at the carrier angular frequency ω_0 of the pulse, and $R(\tau)$ is the nonlinear response function.

The coefficients δ_m from the second order to the fourth order are expressed as

$$\delta_2 = \frac{\beta_2}{2\gamma P_0 T_0^2} = -\frac{1}{2}\frac{\lambda_0^2}{2\pi c}\frac{D_0}{\gamma P_0 T_0^2}\left(1-\frac{\xi}{\gamma P_0 L_0}\right) \tag{5}$$

$$\delta_3 = \frac{\beta_3}{6\gamma P_0 T_0^3} = \frac{1}{3}\frac{\lambda_0^3}{(2\pi c)^2}\frac{D_0}{\gamma P_0 T_0^3}\left(1-\frac{\xi}{\gamma P_0 L_0}\right) \tag{6}$$

$$\delta_4 = \frac{\beta_4}{24\gamma P_0 T_0^4} = -\frac{1}{24}\frac{\lambda_0^4}{(2\pi c)^3 \gamma P_0 T_0^4} \cdot \left[\lambda_0^2 D_2 + 6D_0\left(1-\frac{\xi}{\gamma P_0 L_0}\right)\right] \tag{7}$$

When propagation distance z is near zero, Eq. (4) is dominated by the second-order term

$$-\frac{1}{2}\frac{\lambda_0^2}{2\pi c}\frac{D_0}{\gamma P_0 T_0^2} \tag{8}$$

When z is near L_0, Eq. (4) is dominated by the fourth-order term

$$-\frac{1}{24}\left(\frac{\lambda_0^2}{2\pi c}\right)^3 \frac{D_2}{\gamma P_0 T_0^4} \tag{9}$$

From the above results, we define three dimensionless parameters

$$\begin{aligned} \Delta_0 &= \frac{\lambda_0^2}{2\pi c}\frac{D_0}{\gamma P_0 T_0^2} \\ \Delta_2 &= \left(\frac{\lambda_0^2}{2\pi c}\right)^3 \frac{D_2}{\gamma P_0 T_0^4} \\ \xi_0 &= \gamma P_0 L_0 \end{aligned} \tag{10}$$

The normalized parameter Δ_2 which corresponds to the real parameters D_2 is defined as the normalized quadratic dispersion coefficient. The normalized parameter ξ_0 which corresponds to the real parameter L_0 is defined as the normalized effective fiber length. The normalized parameter Δ_0 coincides with the real parameters $1/N^2$, where N is the soliton order, defined as

$$N = (\gamma P_0 T_0^2 / |\beta_2|)^{1/2} \tag{11}$$

We expect the output SC spectrum from a DFDF to be uniquely specified by three normalized parameters N, Δ_2 and ξ_0.

The input pulses are assumed to have the form

$$U(0,\tau) = \mathrm{sech}(\tau) \tag{12}$$

2 Numerical results and discussion

2.1 Typical SC generation in DFDFs

We first demonstrate typical SC generation in DFDFs. Fig. 1 shows the generated SC spectra which are uniquely specified by the normalized parameters N, Δ_2 and ξ_0. The parameters are set to be $N=2$, $\Delta_2 = -2\times10^{-6}$ and $\xi_0 = 3.50$. The spectra are observed at a normalized propagation distance of $\xi = 1.1\xi_0$ (corresponding to the real propagation distance of $z = 1.1L_0$). The effect of fiber loss is not included.

Fig. 1(a) and (b) show a constant pulse duration $T_{\mathrm{FWHM}} = 4$ ps and various peak powers for the pump pulse. For Fig. 1(a), $\gamma P_0 = 9.9\ \mathrm{km}^{-1}$, $D_0 = 10$ ps/(nm/km), $D_2 = -2.5\times10^{-4}$ ps/(nm^3/km) and $L_0 = 0.354$ km. For Fig. 1(b), $\gamma P_0 = 29.7\ \mathrm{km}^{-1}$, $D_0 = 30$ ps/(nm/km), $D_2 = -7.5\times10^{-4}$ ps/(nm^3/km) and $L_0 = 0.118$ km. These results show identical spectra, which have the -27 dB bandwidth of 250 nm. Spectrum of Fig. 1(c) shows a pulse duration $T_{\mathrm{FWHM}} =$ 8ps for the pump pulse. For Fig. 1(c), $\gamma P_0 = 4.95\ \mathrm{km}^{-1}$, $D_0 = 20$ ps/(nm/km), $D_2 = -2.0\times10^{-3}$ ps/(nm^3/km) and $L_0 = 0.708$ km. The -27 dB bandwidths of spectrum in Fig. 1(c) is 125 nm. These spectra have the same shape, and the bandwidths are inversely proportional to the duration of a pump pulse T_{FWHM}. The above results show that the shape of a spectrum is uniquely specified by the normalized parameters N, Δ_2 and ξ_0.

The most notable feature of Fig. 1 is that the generated SC spectra are accompanied by a strong spectral peak covering the pump wavelength range. The strong spectral peak is the residual pump component which is the most typical characteristic of the SC spectra generated from DFDFs.

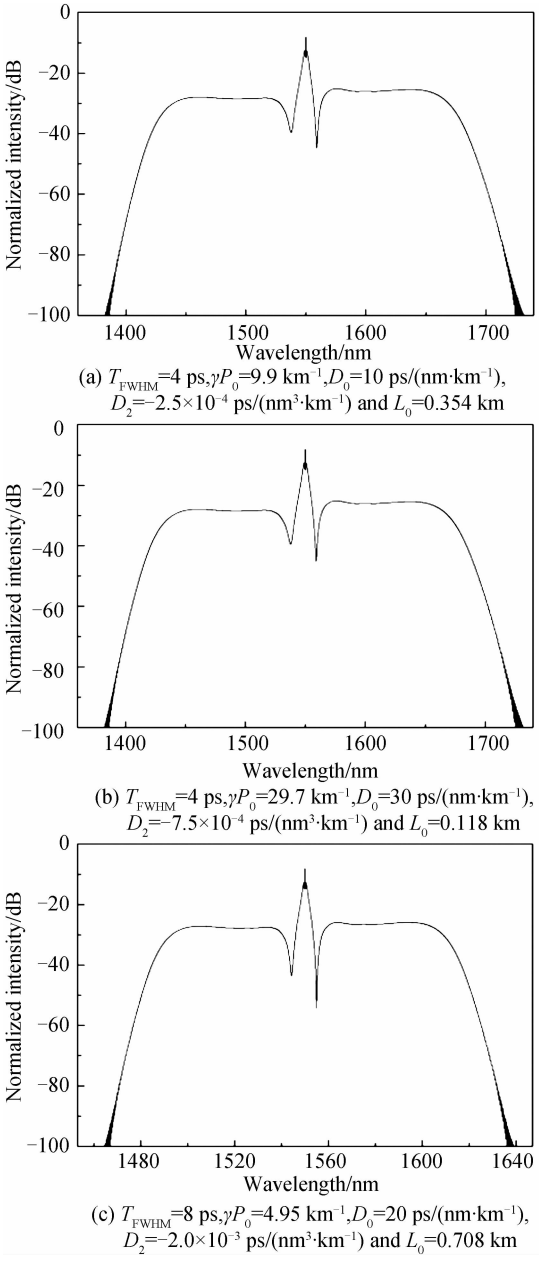

(a) T_{FWHM}=4 ps, γP_0=9.9 km^{-1}, D_0=10 ps/(nm·km^{-1}), D_2=-2.5×10^{-4} ps/(nm^3·km^{-1}) and L_0=0.354 km

(b) T_{FWHM}=4 ps, γP_0=29.7 km^{-1}, D_0=30 ps/(nm·km^{-1}), D_2=-7.5×10^{-4} ps/(nm^3·km^{-1}) and L_0=0.118 km

(c) T_{FWHM}=8 ps, γP_0=4.95 km^{-1}, D_0=20 ps/(nm·km^{-1}), D_2=-2.0×10^{-3} ps/(nm^3·km^{-1}) and L_0=0.708 km

Fig. 1 Typical SC spectra generated from DFDFs specified by the normalized parameters $N=2$, $\Delta_2 = -2\times10^{-6}$ and $\xi_0 = 3.50$

The process of SC generation in DFDF is an interplay between nonlinear and dispersive effects. SC generation in the DFDF consists of two stages: pulse compression and spectral shaping. In the anomalous dispersion segment of the fiber, the adiabatically decreasing dispersion induces an initial phase of symmetrical spectral broadening and associated temporal compression. After a propagation distance of around L_0, the spectral bandwidth increases sufficiently to induce dispersive wave generation symmetrically with respect to the pump wavelength. After propagating beyond L_0 when the dispersion is normal everywhere, the residual pump components temporally broaden and overlap with the frequency-shifted dispersive waves, facilitating interaction through cross-phase modulation. The combined result of these dynamics leads to a broad and flat SC spectrum generation.

The problem with the typical spectra generated from DFDFs is that much of the pump pulse energy is stored in the strong residual pump components. Fig. 2 shows the corresponding compressed SC pulse at the normalized propagation distance of $\xi = 0.95\xi_0$. It is evident that the compressed pulse consists of a narrow spike accompanied by a broad pedestal component. The energy contained in the pedestal component exceeds 45%, as a result, the spectrally flat region of the output SC spectrum is quite low in power.

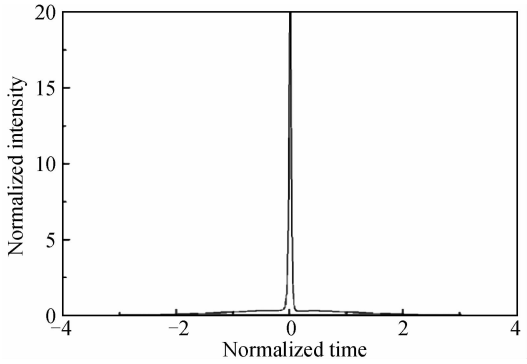

Fig. 2 The corresponding compressed SC pulse at the normalized propagation distance of $\xi=0.95\xi_0$

2.2 Residual pump component suppression

According to the results presented in Fig. 1, the shape of the SC spectrum is determined by the normalized parameters N, Δ_2 and ξ_0. For a given N and a given Δ_2, we can optimize ξ_0 to improve distribution of pump power among the SC spectrum. There exists an optimal value of ξ_0 that suppresses the residual pump component to the utmost extent meanwhile the SC spectrum keeps good spectral flatness.

Now we present the calculation of the optimal value of ξ_0. To estimate the fluctuation of the SC spectrum, we introduce the following factor

$$S = \int_{\lambda_1}^{\lambda_2} [I(\lambda) - I_{\min}]\mathrm{d}\lambda \tag{13}$$

where λ is the wavelength, $I(\lambda)$ is the spectrum intensity, $I_{\min}$ is the minimum value of $I(\lambda)$ for λ in the range of $\lambda_1<\lambda<\lambda_2$. The smaller the value of S-factor, the flatter the SC spectrum. If a spectrum has strong spectral peak or deep groove, the value of S-factor will be very large. For a spectrum with ideal spectral flatness, the value of S-factor tends to zero.

In the numerical simulations, we changed the parameter ξ_0 and fixed other parameters (input soliton order N, and parameter Δ_2) in order to observe the effect of ξ_0. As a result, the S-factor of the output spectrum depends on ξ_0. In this work, we aim to describe the suppression of residual pump component, so λ_1 and λ_2 are set close to the pump wavelength λ_p. In the calculations, we set $\lambda_2-\lambda_p=\lambda_p-\lambda_1=20$ nm.

We kept the parameter Δ_2 constant at -2×10^{-6} and calculated the curve of S-factor for values of input soliton order N in the range $1.0\leqslant N\leqslant2.2$. Fig. 3 shows the S-factor curves for six typical input soliton orders of $N=2.0$, 1.7, 1.5, 1.3, 1.1 and 1.0, respectively. For each input soliton order N, the parameter ξ_0 begins from its threshold value ξ_{th} defined as the normalized propagation distance at which we obtain the typical SC spectrum, as is shown in Fig. 1. There several notable features in the figures. First, the threshold value ξ_{th} increases as the input soliton order N decreases. Second, when $\xi_0=\xi_{\text{th}}$, the S-factor has a maximum value. Third, the curves of S-factor consist of many peaks and troughs. Both the peak values and the trough values of the curves tend to decrease as ξ_0 increases. When ξ_0 exceeds a certain value, the trough value of the S-factor curves will reach a minimum value (indicated by A or B). The normalized parameter ξ_0 corresponding to point A and point B are indicated as ξ_A and ξ_B, respectively. In the calculations, we found that when $N>1.7$, the value of point A is slightly smaller than that of point B. When $N<1.7$, the curve has a relative minimum value at point B.

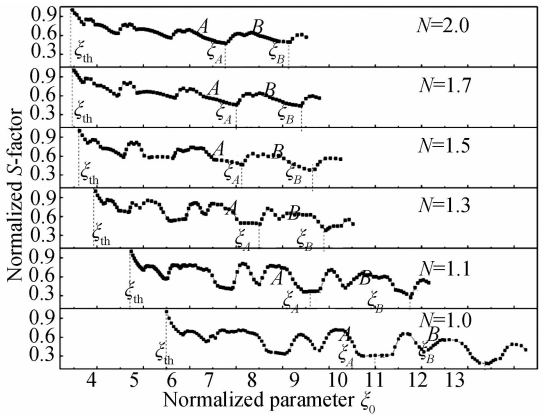

Fig. 3 Calculated S-factor of the output SC spectrum as a function of ξ_0

Fig. 4 (a) and (b) show two group SC spectra which are generated at ξ_A and ξ_B (as indicated in Fig. 3), respectively. It is worth noting that all curves in Fig. 4 are to the same scale but displaced vertically for the sake of clarity. Compared with the SC spectra in Fig. 1, both of two group SC spectra in Fig. 4 have good spectral flatness and the spectrally flat region significantly extend. For the same input soliton order N, there are still some small differences between the two spectra. As seen in Fig. 4, when $N>1.7$, the flatness of the spectra generated at ξ_A is slightly better. On the contrary, when $N<1.7$, the flatness of the spectra generated at ξ_B is slightly better. The results confirm that the smaller the value of S-factor, the flatter the generated spectrum.

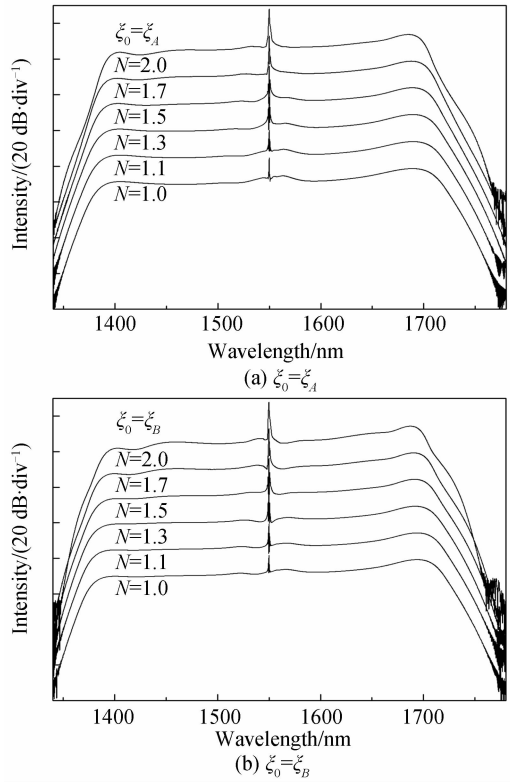

Fig. 4 The SC spectra generated at ξ_A and ξ_B

Although the SC spectra in Fig. 4 still contain a spectral peak due to higher-order soliton compression, the spectral peak obviously becomes narrow and the power variation of the residual pump components have been suppressed greatly. From Fig. 4, we can see clearly that as input soliton order N decreases, the spectral peak becomes narrower and its intensity becomes lower. For $N=1$ (a fundamental soliton), the residual pump component is suppressed to the utmost extent, while the SC spectrum keeps good spectral flatness.

Fig. 5 shows the calculated ξ_A and ξ_B as a function of input soliton order N. The curves indicate that the variations of ξ_A and ξ_B with N follow the similar pattern. As the input soliton order N decreases, both of ξ_A and ξ_B increase. When N decreases down to <1.4 ($N<1.4$), the rate of increase becomes larger. For a lower-order soliton, to generate an optimum SC spectrum the required optimal ξ_0 is large. For the same input soliton order N, the value of ξ_A is obviously less than that of ξ_B. As there are only minor differences between the spectra generated at ξ_A and ξ_B, so we can choose ξ_A as the optimal value of ξ_0. If ξ_0 is set in the vicinity of ξ_A, we can obtain a desirable SC spectrum with a relatively low ξ_0.

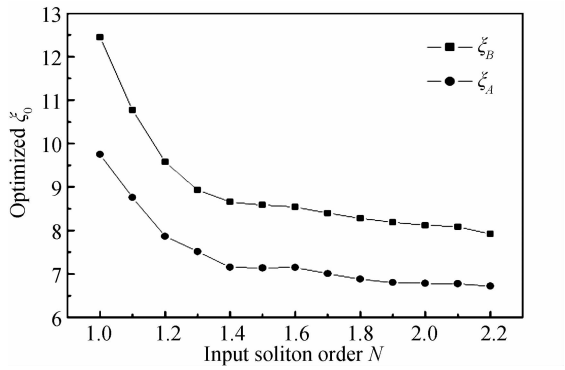

Fig. 5 Calculated ξ_A and ξ_B as a function of input soliton order N

We chose ξ_A as the optimal value of ξ_0 and calculated the proportion of pedestal energy of the compressed SC pulse at the normalized propagation distance of $\xi=0.95\xi_A$. Fig. 6 shows the pedestal energy of the compressed SC pulse as a function of input soliton order N. It can be seen that as N decreases, the pedestal energy tends to decreases. The tradeoff for minimizing the energy of residual pump component is the decrease of input soliton order N and the increase of optimal ξ_A. We note that, when N decreases down to <1.2 ($N<1.2$), the proportion of pedestal energy decreases down to less than 6%.

To understand the evolution of a SC pulse, it is instructive to examine the evolution of the soliton order of the SC pulses along the length of the DFDFs. Fig. 7 shows the evolution of the soliton order before the normalized propagation distance of ξ_0 (we chose $\xi_0=\xi_A$, as is shown in Fig. 5) for input soliton order $N=2.0$, 1.7, 1.5, 1.3, 1.1 and 1.0, respectively, which correspond to the cases shown in Fig. 4(a). The value of ξ_0 for each N can be obtained from Fig. 5. In the case of $N>1.1$, the soliton order rapidly decreases down to <1 ($N<1$) in the initial stage of propagation, and then fluctuates around the value of 1. The SC pulse eventually evolves toward a fundamental soliton before the normalized distance of ξ_0. A part of the pulse energy is dispersed away in the process. With further evolution toward the normalized distance of ξ_0, the dispersion at the pump wavelength tends to zero, and the soliton order rapidly increases. In contrast, in the case of $N=1$ and $N=1.1$, the soliton order of the SC pulses changes

slightly in the initial stage of propagation, and then gradually evolves toward a fundamental soliton. Thus it can be concluded that SC pulse propagation in DFDF before the normalized distance of ξ_0 is a process of transforming an input soliton into a fundamental soliton. Therefore, to obtain a flat SC spectrum with weak residual pump component, an input pulse with N close to 1 is recommended.

Numerical simulations under different parameters such as normalized parameter Δ_2 and pulse duration T_{FWHM} obtained similar results.

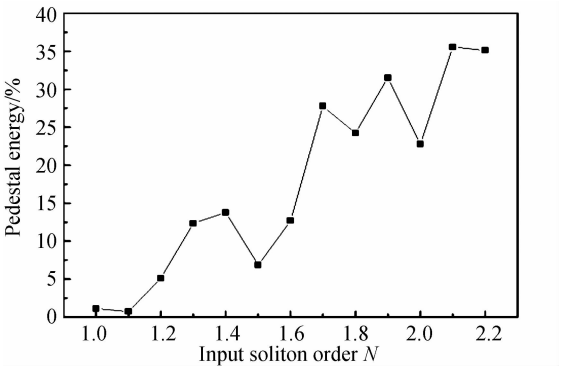

Fig. 6 Calculated pedestal energy of the compressed SC pulse at $\xi=0.95\xi_A$ as a function of input soliton order N

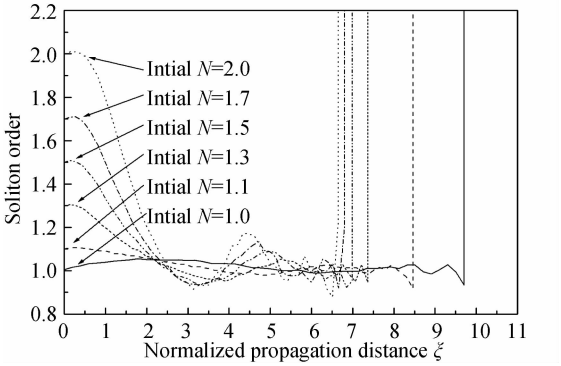

Fig. 7 Evolution of soliton order of the SC pulses along the propagation distance before $\xi=\xi_0$

3 Conclusion

A technique for suppressing residual pump component of SC spectrum generated in DFDFs has been presented. For a pump pulse with a given N and a given Δ_2, by optimizing the normalized parameter ξ_0, the residual pump component can be suppressed effectively and a more even distribution of pump power among the generated wavelengths can be achieved. The optimal value of ξ_0 for generating an optimum SC spectrum depends on N and Δ_2. When N decreases, the optimal value of ξ_0 increases and the pedestal energy of the compressed SC pulse tends to decrease. To realize high quality residual pump component suppression, the pedestal energy of the compressed SC pulse must be minimized. To obtain a flat SC spectrum with weak residual pump component, an input pulse with N close to 1 is recommended.

Reference

[1] ZHANG Li-jia, XIN Xiang-jun, Liu Bo, *et al*. OFDM modulated WDM-ROF system based on PCF-Supercontinuum [J]. *Optics Express*, 2010, **18**(14): 15003-15008.

[2] HULT J, WATT R S, KAMINSKI C F. High bandwidth absorption spectroscopy with a dispersed supercontinuum source [J]. *Optics Express*, 2007, **15**(18): 11385-11395.

[3] KAMINSKI C F, WATT R S, ELDER A D, *et al*. Supercontinuum radiation for applications in chemical sensing and microscopy [J]. *Applied Physics B: Lasers and Optics*, 2008, **92**(3): 367-378.

[4] HARTL I, LI X D, CHUDOBA C, *et al*. Ultrahigh-resolution optical coherence tomography using continuum generation in an air-silica microstructure optical fiber [J]. *Optics Letters*, 2001, **26**(9): 608-610.

[5] MORI K, TAKARA H, KAWANISHI S. Analysis and design of supercontinuum pulse generation in a single-mode optical fiber [J]. *Journal of the Optical Society of America B*, 2001, **18**(12): 1780-1792.

[6] JIN Wei, XU Wen-cheng, CHEN Zhao-xi, *et al*. Effects of dispersion characteristics on supercontinuum generation in dispersion flattened-decreasing fiber [J]. *Acta Optical Sinica*, 2005, **25**(1): 6-10.

[7] XU Wen-Cheng, GAO Jie-Li, LIANG Zhan-Qiang, *et al*. Supercontinuum spectra generation in the single-mode optical fibre with concave dispersion profile [J]. *Chinese Physics*, 2006, **15**(4): 715-720.

[8] GENTY G, COEN S, DUDLEY J. M. Fiber supercontinuum sources [J]. *Journal of the Optical Society of America B*, 2007, **24**(8): 1771-1785.

[9] CHEN Yong-zhu, LI Yu-zhong, XU Wen-cheng. Research on flat ultra-wideband supercontinuum generated in dispersion-flattened decreasing fiber [J]. *Acta Physica Sinica*, 2008, **57**(12): 7693-7698.

[10] CHEN Yong-zhu, YU Zhi-qiang. Ultra-wideband supercontinuum generation in a fiber with convex dispersion profile [J]. *Semiconductor Optoelectronics*, 2009, **30**(2): 268-272.

[11] JIANG Guang-yu, HUANG Yan, WAN Sheng-peng, *et al*. Numerical simulation and optimization of supercontinuum generation in dispersion decreasing fiber [J]. *Acta Photonica Sinica*, 2009, **38**(9): 2318-2324.

[12] KAKKAR C, THYAGARAJA N. Design optimisation for obtaining flat, high power supercontinuum source over C + L band [J]. *Optics Express*, 2006, **14**(22): 10292-10297.

[13] HAN Ying, HOU Lan-tian, ZHOU Gui-yao, *et al*. Flat supercontinuum generation within the telecommunication wave bands in a photonic crystal fiber with central holes [J]. *Chinese Physics Letters*, 2012, **29**(5): 054208.

[14] ZHU Xian, ZHANG Xin-ben, CHEN Xiang, *et al*. Blue-extended supercontinuum generation in photonic crystal fibers with picosecond pulsepumping [J]. *Chinese Physics Letters*, 2012, **29**(12): 124210.

[15] YUAN Jin-hui, SANG Xin-zhu, YU Chong-xiu, *et al*. Broad and ultra-fattened supercontinuum generation in the visible wavelengths based on the fundamental mode of photonic crystal fibre with central holes [J]. *Chinese Physics B*, 2011, **20**(5): 054210.

[16] AGRAWAL G P. Nonlinear fiber optics [M]. Singapore: Academic Press, 2009.